Journal of Applied Polymer Science

Improving the Thermal and Mechanical Properties of Poly(vinyl butyral) Through the Incorporation of Acid-Treated Single-Walled Carbon Nanotubes

Ali Reza Zanjanijam,[1,2] Morteza Hajian,[1] Gholam Ali Koohmareh[1]
[1]Department of Chemistry, University of Isfahan, Isfahan 81746-73441, Iran
[2]Engineering Faculty, Iran Polymer and Petrochemical Institute, Tehran 14965-115, Iran
Correspondence to: A. R. Zanjanijam (E-mail: a.zanjani@ippi.ac.ir)

ABSTRACT: In this study, to investigate the effect of functionalized carbon nanotubes on the thermal and mechanical properties of the poly(vinyl butyral) (PVB) resin, PVB/functionalized single-walled carbon nanotube (f-SWCNT) composites were fabricated by a solution casting method. The functionalized nanotubes were prepared by acid treatment. The formation of oxygen-containing functional groups on the surface of the nanotubes was confirmed by Fourier transform infrared spectroscopy, energy-dispersive X-ray spectroscopy, and scanning electron microscopy (SEM) measurements. SEM analysis also showed that the nanotubes were dispersed well in the PVB matrix. The thermal stability of the composites were investigated with thermogravimetric analysis, and the results show better stability for PVB in the presence of a very low content of the f-SWCNTs. The prepared composites exhibited a significant increase in the temperature of degradation at 50 wt % loss and also in the onset temperature and decomposition temperature at the maximum rate of weight loss of butyral degradation. A significant enhancement in the mechanical properties was also achieved for these prepared composites. © 2014 Wiley Periodicals, Inc. J. Appl. Polym. Sci. **2014**, *131*, 40481.

KEYWORDS: composites; mechanical properties; nanotubes; thermal properties

Received 3 October 2013; accepted 20 January 2014
DOI: 10.1002/app.40481

INTRODUCTION

Carbon nanotubes are one of the best nanofillers for reinforcing polymers. Calculations and experimental data have indicated that the nanotubes have excellent mechanical and thermal properties, including a high tensile strength (50–200 GPa) and Young's modulus (1.2 TPa).[1] These properties make nanotubes a favorite nanofiller for reinforcement in polymer composites.

The efficiency of these nanotubes in the enhancement of the mechanical and other properties of composites depends on the dispersion degree of the filler in the polymer matrix and interactions between the polymer and the nanotubes. Carbon nanotubes, especially single-walled carbon nanotubes (SWCNTs), are in the form of bundled structures or ropes and tend to agglomerate because of van der Waal's forces. So, it is difficult to disperse them well in a polymer matrix.[2]

It seems that the functionalization of the nanotubes is the best way to prevent nanotube aggregation. Functionalization causes better dispersion of the nanotubes in solvents and polymer matrices and higher stress–strain transfer between the filler and the polymer. This is more pronounced in the case of the solution casting technique because good dispersion of the nanotubes in the solvent prevents the aggregation of the filler in the polymer.[3–5] Functionalization methods can be classified into covalent and noncovalent functionalization.[6] The most common method for covalent functionalization of nanotubes is oxidation. Different functional groups, such as carboxylic acid and alcohol groups, are formed on the surface of the nanotubes during the oxidation by various oxidizing reagents, such as nitric acid, sulfuric acid, and their mixtures.[7,8]

The extent of the carboxylic group formation on the surface of the nanotubes relies on the time, temperature, and procedure of the oxidation.[9,10] Functionalized nanotubes are very stable in polar solvents. For instance, it has been reported that acid-treated nanotubes were stable in water for more than 3 months.[11]

Poly(vinyl butyral) (PVB) is prepared by a condensation reaction between poly(vinyl alcohol) (PVA) with butanal. PVB shows good adhesion to many surfaces, especially glass, and has a high toughness and flexibility. It has been used in many applications, such as in the manufacturing of safety glasses, coatings, wash primers and print inks.[12–14]

Many studies have demonstrated remarkable increases in the mechanical properties through the addition of functionalized

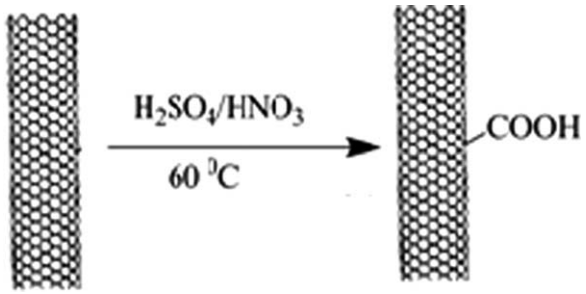

Figure 1. Schematic presentation for the functionalization of the SWCNTs.

carbon nanotubes for different composites, in particular, composites fabricated by the solution casting method.[15] For example, acid-treated nanotubes enhanced the tensile strength of PVA and polycaprolactone by 117 and 12.15%, respectively.[11,16] Also, the reinforcement of polyurethane with 10 wt % carboxylated multiwalled carbon nanotubes resulted in a 108% increase in the tensile strength of the polymer.[17]

Carbon nanotubes can also retard the thermal degradation of polymers and enhance their thermal stability and flammability properties. For example, thermogravimetric analysis (TGA) showed that in the incorporation of nanotubes in polypropylene, the decomposition temperature at the maximum rate of the weight loss (T_{max}) of the composite was shifted to a higher temperature by 12°C.[18]

Recently, the preparation and characterization of PVB/graphene composites was reported by our group,[19] and in continuation of our research on PVB and its composites, now, we report the influence of functionalized single-wall carbon nanotubes (f-SWCNTs) on the thermal and mechanical properties of PVB composites. First, the SWCNTs were modified with an oxidation method, and then, PVB composites filled with f-SWCNTs were prepared by a solution casting technique. The aim of this study was to evaluate the thermal degradation behavior and mechanical properties of PVB in the presence of the f-SWCNTs.

EXPERIMENTAL

Materials

The SWCNTs were supplied by the Oil Industry Institute of Iran. These carbon nanotubes had a diameter of 2 nm, a length of some micrometers, and a purity greater than 95%, as reported by the producer. PVA, with a molecular weight of 72.000 g/mol, was provided from Appli Chemical Co., and butanal was supplied by Aldrich. Other chemicals were obtained from Merck and were used without additional treatment. The PVB (the polymer matrix) was prepared by a process presented in our previous study.[19]

Functionalization of the SWCNTs

SWCNTs and 30 mL of concentrated sulfuric acid were stirred for 5 min at room temperature, and then, 15 mL of concentrated nitric acid was added to this solution slowly. It was heated for 12 h at 60°C. The mixture was then cooled, and water was added to the solution. The resulting mixture was filtered, washed with HCl (5%) and water, and dried at 70°C for 24 h. The schematics of the nanotube functionalization by the oxidation method is shown in Figure 1.

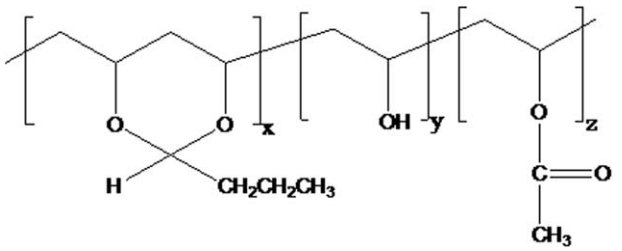

Figure 2. Chemical structure of PVB.

Synthesis of the PVB/f-SWCNT Nanocomposites

To investigate the influence of the modified SWCNTs on the various properties of the polymeric matrix, PVB/f-SWCNT composites were fabricated by the solution casting method. A mixture of f-SWCNTs, sodium dodecyl sulfate (SDS) and ethanol were sonicated for 1 h. The concentration of the nanotubes in suspension was 0.1 mg/mL and ratio of the SDS to f-SWCNTs was 10:1. The resulted suspension was added to a mixture of the PVB (1.6 g) and tri(ethylene glycol) bis(2-ethyl hexanoate) (0.4 g) in ethanol (30 mL) which was made at 60°C. The mixture was then agitated for 1 h and composite films containing 0.6 and 0.9 wt % f-SWCNTs were obtained by pouring the solution in a mold and evaporating the solvent at ambient temperature for overnight.

Characterization and Property Measurements

Fourier transform infrared (FTIR) spectra for the characterization of functional groups in the pristine SWCNTs and f-SWCNTs were recorded by a Jasco FTIR-6300 spectrometer. The surface morphology of the SWCNTs before and after the functionalization process and also that of the PVB/f-SWCNT composites were evaluated by an AIS-2100 model 550 Seron Technology scanning electron microscope equipped with an energy-dispersive X-ray spectroscopy (EDS) system. The thermal stability of the pure PVB and prepared nanocomposites were investigated with a Setaram Labsys thermogravimetric (TG) system from ambient temperature to 600°C at a heating rate of 10°C/min under a nitrogen atmosphere. The differential scanning calorimetry (DSC) measurements were performed with the Setaram Labsys TG system at a heating rate of 10°C/min. The tensile properties were measured on dumbbell-shaped samples cut from the films by a Santam Co. model SMT5 at room temperature. The film thickness and strain rate were 0.23 mm and 50 mm/min, respectively. For each sample, four measurements were made.

RESULTS AND DISCUSSION

Characterization of the PVB

The PVB was synthesized by the reaction of PVA with butanal. The chemical structure of PVB is shown in Figure 2. In the acetalization reaction, neighbor hydroxyl groups reacted with each other, and a butyral ring formed. The FTIR spectrum of the PVA is shown in Figure 3. In this spectrum, the O—H and C—O stretching vibrations appeared at 3450 and 1095 cm^{-1}, respectively. After the reaction with butanal, the hydroxyl

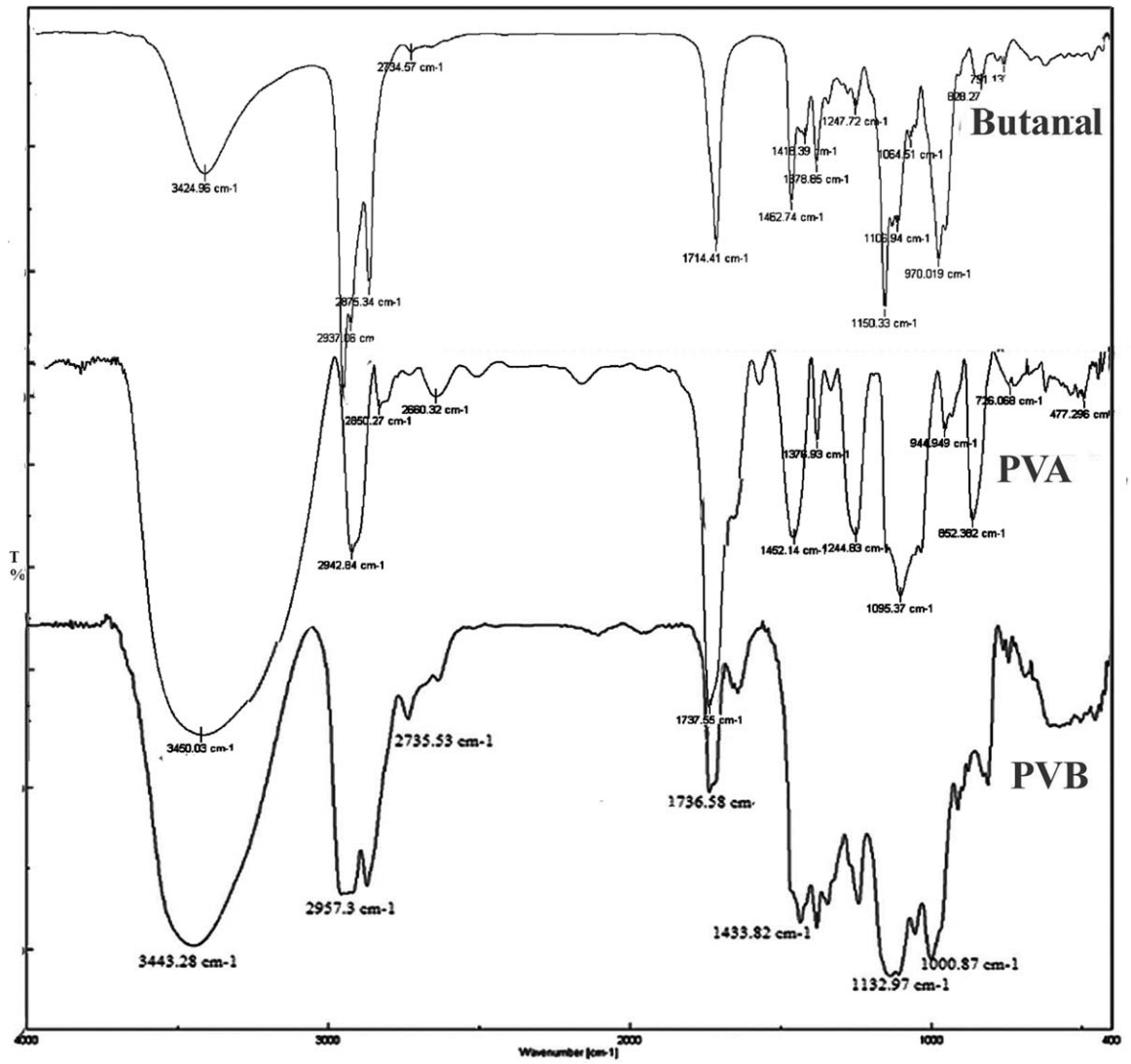

Figure 3. FTIR spectra for butanal, PVA, and PVB.

functional groups changed into a butyral ring. A comparison between the FTIR spectra of the PVA and PVB (Figure 3) showed two new absorption peaks at 1017 and 1132 cm^{-1}, which corresponded to the asymmetric and symmetric stretching vibrations of C—O—C (butyral ring).[12,13,20] Also, because of the acetalization reaction, the O—H peak intensity in the 3400-cm^{-1} region decreased.[12]

Also, in the case of the aliphatic C—H stretching vibrations, there was no any sharp increase in the intensity of the peak after the reaction. In the PVA spectrum, the transmittance percentage for this peak was 60%, whereas in the PVB spectrum, the transmittance percentage was 65%.

Characterization of the f-SWCNTs

To improve the dispersion of the nanotubes in the PVB matrix and good interaction between the nanofiller and polymer matrix, the SWCNTs were functionalized by the oxidation method. We discovered this by observing the FTIR spectra and EDS data in which acidic and alcoholic functional groups were created on the tail end and defect points of the nanotubes. Figure 4 shows the FTIR spectra of the pristine SWCNTs and f-SWCNTs. As shown in this figure, after the functionalization step, a broad peak corresponding to O—H stretching vibrations from 3000 to 3600 cm^{-1} appeared. In addition, the stretching vibrations of C═O at 1721 cm^{-1} were observed. These were attributed to the presence of carboxylic acid functional groups. The formation of C—O bonds (the peak at 1057 cm^{-1}) also proved the acid functionalization of the nanotubes.[21,22]

Elemental analysis of the pristine and functionalized carbon nanotubes was measured with EDS. Figure 5 shows the EDS spectra for the pristine SWCNTs and f-SWCNTs, respectively. Also, in Table I, the EDS data, including the peak intensity and weight percentage of the elements for two groups of nanotubes, are presented. As shown in Table I, the contents of carbon (graphitic and amorphous) and oxygen in the pristine SWCNTs were 82.70 and 14.68 wt %, respectively. This sample also contained a small amount of cobalt (catalyst remaining) and sulfur. The data indicated that a higher content of oxygen for the f-

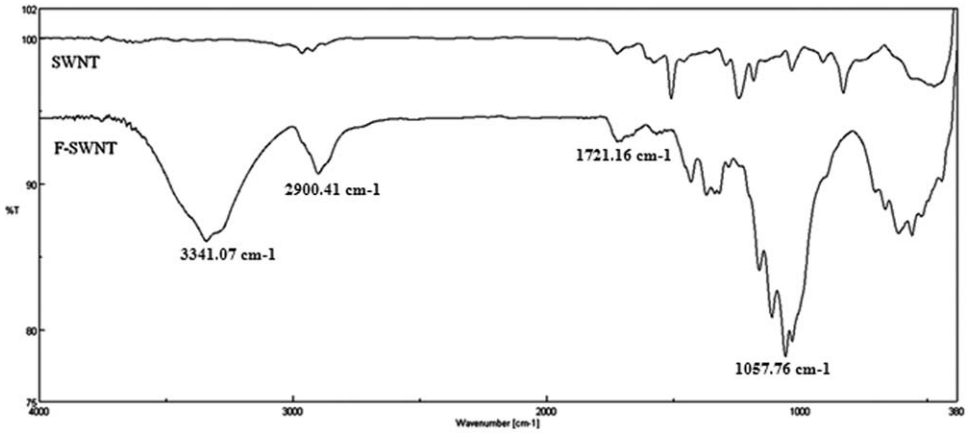

Figure 4. FTIR spectra for the pristine SWCNTs and f-SWCNTs.

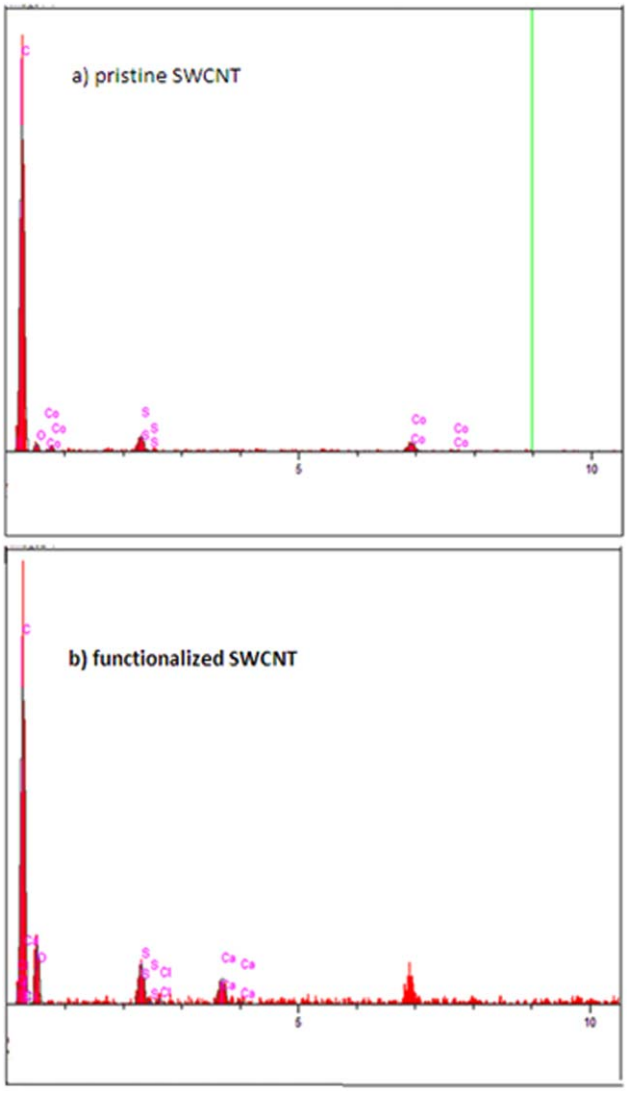

Figure 5. EDS spectra of the (a) pristine SWCNTs and (b) f-SWCNTs. [Color figure can be viewed in the online issue, which is available at wileyonlinelibrary.com.]

SWCNTs was achieved. In this sample, the oxygen weight percentage increased to 37.19 wt %. As shown, the atomic ratio of O/C increased significantly after oxidation by acids. The cobalt elimination in these nanotubes (that related to the purification by acids) also was outcome of the oxidation process. By comparison of the EDS spectra and the resulting data and the FTIR spectra, we concluded that the oxygen-containing functional groups, such as the carboxylic acid, were formed successfully on the surface of the nanotubes.

Morphological Properties

Scanning electron microscopy (SEM) images from the surfaces of the SWCNTs and f-SWCNTs are shown in Figure 6. Figure 6(a) shows that the pristine SWCNTs were in agglomerated form. This was due to the strong van der Waal's interactions between the individual SWCNTs, which caused their entanglement. After functionalization, the nanotubes were freed from the entanglements and had a high aspect ratio because of presence of the functional groups on their surface [Figure 6(b)]. These images indicate the important role of the nanotube functionalization on the dispersion of the SWCNTs and the prevention of their aggregation.

Table I. EDS Data for the Pristine SWCNTs and f-SWCNTs

Element	Intensity (c/s)	wt %
Before functionalization		
C	399.61	82.70
O	9.71	14.68
S	23.51	0.99
Co	18.48	1.64
After functionalization		
C	101.27	60.00
O	17.73	37.19
S	15.64	1.45
Cl	2.19	0.21
Ca	12.03	1.15

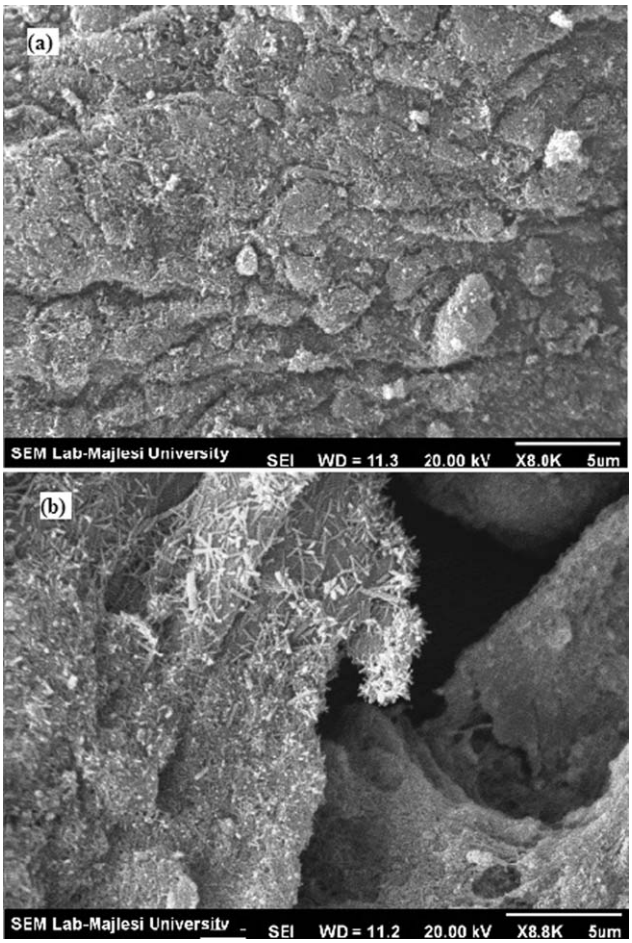

Figure 6. SEM micrographs of the (a) pristine SWCNTs and (b) f-SWCNTs.

The dispersion quality of the f-SWCNTs in the prepared composites was evaluated by SEM. Figure 7(a) is the SEM micrograph of the PVB/f-SWCNT composite with a nanotube content of 0.6 wt %. The SEM micrograph shows that the f-SWCNTs were effectively dispersed in the PVB matrix. The carboxylic acid and alcoholic groups seemed to enhance the dispersion of the SWCNTs by higher interactions with the functional groups of the PVB matrix. This could be ascribed to the high polarity of the oxygen-containing functional groups, which increased adhesion between the nanotubes and the PVB matrix. We expected that the functionalization of the SWCNTs would boost load transfer from the PVB matrix to the nanotubes and, hence, improve the mechanical behavior of the fabricated samples. In Figure 7(b), the SEM micrograph for PVB/0.9 wt % f-SWCNTs is shown. In this composite, the nanotubes were in agglomerated from and adverse dispersion was seen. This resulted from the high loading of the filler and attractive forces between the SWCNTs.

Thermal Degradation

TGA Studies. TGA was applied to measure the degradation behavior of the PVB and corresponding nanocomposites. The analyses were carried out from ambient temperature to 600°C at a heating rate of 10°C/min under an N_2 atmosphere. The TGA and derivative TG thermograms of the neat polymer and the composites filled with functionalized nanotubes are compared in Figures 8 and 9.

TGA showed that there was two-step decomposition for the PVB. The first step was the degradation of hydroxyl groups at temperatures between 200 and 300°C, and the second one was correlated with the decomposition of butyral at temperatures higher than 300°C. The thermal degradation of the PVB in a nitrogen atmosphere resulted in the release of the water, butanal, and acetic acid. After the thermal degradation of PVB, carbon residue was left behind. The composites contained carbon residue and nanotubes that did not degrade in the nitrogen atmosphere. The main decomposition step in the degradation of the PVB was the elimination of the butyral, and as a result, butanal formed during this step.[23] For the PVB sample prepared in this study, the onset temperature (T_{onset}) of the butyral ring decomposition (the second step of the PVB degradation) and T_{max} in this step were observed at 341 and 393°C, respectively.

From the TGA thermograms (Figure 8), it was obvious that the degradation shifted to higher temperatures, and the thermal stability of the composites improved with addition of the f-SWCNTs into the polymer matrix. The thermal properties data of the PVB/f-SWCNT composites are presented in Table II.

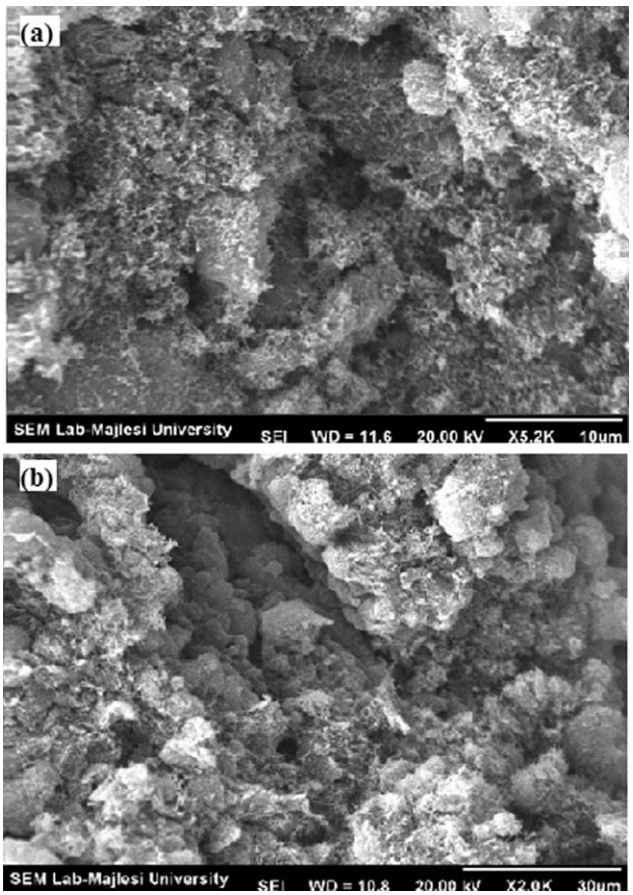

Figure 7. SEM micrographs of composites containing (a) 0.6 and (b) 0.9 wt % f-SWCNTs.

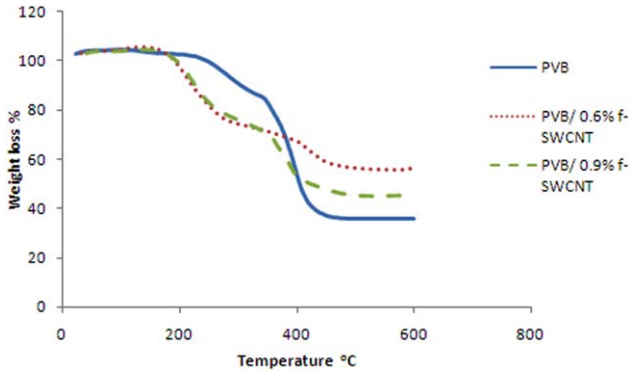

Figure 8. TGA thermograms for the pure PVB and its composites under a nitrogen atmosphere at a heating rate of 10°C/min. [Color figure can be viewed in the online issue, which is available at wileyonlinelibrary.com.]

Also, it can be seen from the TGA thermograms and Table II that the composites filled with 0.6 and 0.9 wt % f-SWCNTs had lower thermal stabilities at 200–300°C. These composites showed lower $T_{5\%}$ and $T_{10\%}$ ($T_{5\%}$ and $T_{10\%}$ are the temperature of degradation at 5 wt. % loss and 10 wt. % loss, respectively) values relative to the neat PVB. This phenomenon was attributed to two major factors; one was the method applied to the preparation of the composites. A solution casting method was used for the fabrication of the neat PVB and PVB/f-SWCNT composites. As mentioned in the Experimental section, the concentration of the nanotubes in suspension was 0.1 mg/mL. The volume of the used solvent was increased through an increase in the f-SWCNTs loading. Drying at room temperature may not have been able to completely remove the residual solvent. The trapped solvent in the composite film (that adsorbed to the PVB chains and polar functional groups of the nanotubes due to hydrogen bonding) gradually diffused from the film and evaporated. The second one may have been due to the degradation of the surfactant, which was used only in the composites for better dispersion of the nanotubes. The thermal degradation of the SDS showed a loss between 160 and 380°C. This phenomenon also was observed in our previous study for PVB/pristine SWCNT nanocomposites.[24]

For the virgin PVB, the temperature of degradation at a 50 wt % loss ($T_{50\%}$) was 403°C. The PVB/0.6 wt % nanotube did not show $T_{50\%}$ because the total amount of the degradation was

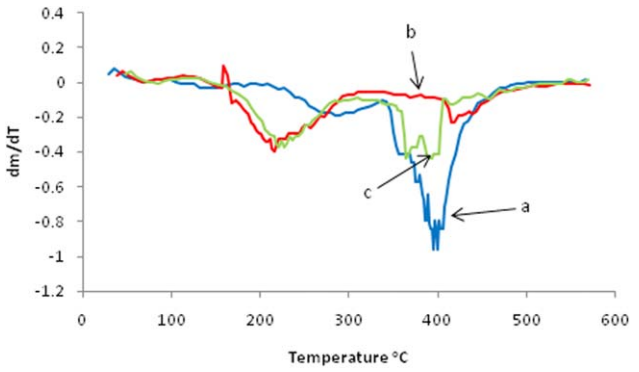

Figure 9. Derivative TG curves for (a) the pure PVB and (b,c) its composites containing 0.6 and 0.9 wt % f-SWCNTs, respectively. [Color figure can be viewed in the online issue, which is available at wileyonlinelibrary.com.]

Table II. Thermal Stability Parameters for the PVB and PVB/f-SWCNT Composites.

Thermal property	PVB	PVB/0.6% f-SWCNTs	PVB/0.9% f-SWCNTs
$T_{5\%}$ (°C)	277	219	216
$T_{10\%}$ (°C)	312	235	228
$T_{50\%}$ (°C)	408	-	412
T_{onset} (°C)[a]	341	402	352
ΔT_{onset} (°C)	-	61	11
T_{max} (°C)[a]	393	414	395
Weight loss in butyral degradation (%)	49.93	10.90	34.85
Residual yield (%)	35.67	55.52	45.42
LOI	31	39	35
ΔH_{comb}	258	205	228

[a] T_{onset} and T_{max} for butyral decomposition. ΔT_{onset} is the difference between Tonset of the composite and neat PVB.

about 45%. For the composite with a 0.9% loading, $T_{50\%}$ was observed at 412°C (Table II). Also, T_{onset} and T_{max} for the decomposition of the butyral increased in the case of the prepared composites; this showed that the thermal degradation of these samples was hindered in the presence of the functionalized nanotubes. T_{onset} of the butyral degradation for the pure PVB and samples loaded with 0.6 and 0.9 wt % f-SWCNT were 341°C, 402°C (an increase of 61°C), and 352°C (an increase of 11°C), respectively. The T_{max} of this degradation step for the PVB was found to be 393°C. The addition of 0.6% nanotubes into the PVB enhanced T_{max} to 414°C whereas this temperature improved only 2°C in the case of the 0.9% content.

The amount of weight lost in this step of degradation significantly decreased for the composites containing 0.6 and 0.9 wt % nanotubes. These values for the neat PVB and the prepared composites were 49.93, 10.90. and 34.85 wt %, respectively. In addition, with the incorporation of the functionalized nanotubes into the PVB matrix, the residual yields of the samples improved remarkably (Table II). This result demonstrated that the thermal degradation process of the PVB was influenced by the presence of the acid-treated nanotubes. The data show that the residual yield of the 0.6% f-SWCNT sample was higher than that of the 0.9% f-SWCNT one. In the sample containing 0.6%, the nanotubes had a better dispersion, and as a result, good interaction between them and the polymeric matrix led to a better stability and a higher residue with respect to the other composite. In fact, the sample filled with 0.9% SWCNTs showed agglomeration of the nanotubes and weak interaction between the carbon nanotubes with PVB. So in this sample, a smaller effect of the nanotubes in stabilizing the polymer was observed.

The char yield (CR; residual mass) could be applied to calculate the limiting oxygen index (LOI) of the PVB and the composites according to the Van Krevelen and Hoftyzer equation:[25–28]

$$LOI = 17 + 0.4CR$$

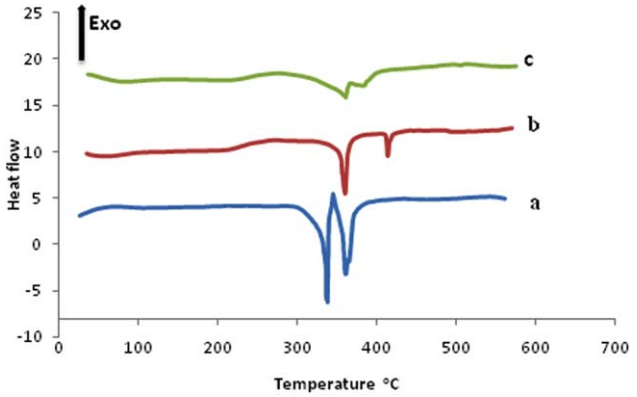

Figure 10. DSC curves for (a) PVB and (b,c) its composites filled with 0.6 and 0.9% functionalized nanotubes, respectively, at a heating rate of 10°C/min. [Color figure can be viewed in the online issue, which is available at wileyonlinelibrary.com.]

The LOI values for the samples was estimated on the basis of the CRs at 600°C. The LOI values for the neat PVB and the composites containing 0.6 and 0.9 wt % were 31, 39, and 35, respectively (Table II). On the basis of the calculated values, all of the samples were considered to be self-extinguishing materials.[29]

According to Johnson,[26–28,30] the specific heat of combustion (ΔH_{comb}) can be predicted by the following equation:

$$\mathrm{LOI} = \frac{8000}{\Delta H_{comb}}$$

This equation is true for materials that have C/O atomic ratios of higher than 6. For the PVB, ΔH_{comb} was 258 J/g, and for the composites, the values decreased to 205 and 228 J/g, respectively (Table II).

The obtained results indicate that the composites filled with functionalized carbon nanotubes had better thermal stability and that the degradation of these samples was remarkably slower than that of the pure PVB. This was attributed to the barrier effect of the SWCNTs. Carbon nanotubes can retard emission of gaseous decomposition products; this results in T_{onset} shifting to higher temperatures. In other words, chains near the SWCNTs might decompose slowly. Also, a high intrinsic thermal conductivity of the nanotubes increased the improvement of the thermal stability. This effect enhanced the dissipation of heat within the polymer matrix. It appeared that strong interfacial adhesion between the polymer matrix and the carbon nanotubes were mainly responsible for the higher thermal stability of the PVB nanocomposites. The good dispersion and high aspect ratio of the individual nanotubes resulted in a significant enhancement in the thermal stability.

As observed in the thermal stability data, the sample with 0.6% f-SWCNTs demonstrated better results in improving the thermal stability of the PVB matrix compared to the sample with 0.9 wt % f-SWCNTs. As mentioned in the morphological properties section, when the nanotube loading reached 0.9 wt %, the agglomeration phenomenon took place, and subsequently, a lower enhancement in the thermal properties was observed. In other words, the ability of the nanotubes to improve the thermal properties relied on a number of factors, including the dispersion degree, aspect ratio, and interfacial adhesion of the nanotubes with the polymer matrix.

DSC Studies. The DSC profiles of the pure PVB and the nanocomposites filled with f-SWCNTs are presented in Figure 10. The PVB sample showed two endothermic peaks at temperatures between 300 and 400°C. The endothermic peaks at 338 and 361°C in the DSC curve of the PVB were due to the removal of the plasticizer and the decomposition of the PVB in a nitrogen atmosphere, respectively. The DSC curve showed that for the virgin PVB, the first peak appeared with a T_{onset} of 335°C and a peak temperature (T_{peak}) of 338°C. The T_{onset} and T_{peak} for the second endothermic peak were 356 and 361°C, respectively. T_{onset} and T_{peak} and also the enthalpy of the both endothermic peaks for all of the samples are summarized in Table III.

In the fabricated composites, T_{onset} and T_{peak} of the both peaks moved to significantly higher temperatures. At 0.6 wt % f-SWCNTs, favorable results were achieved. For this composite, the T_{onset} and T_{peak} were increased 16 and 20°C for the first endothermic peak and 54 and 51°C for the second one (Table III). As shown in Figure 10 and Table III, the enthalpy values also decreased very notably, especially for the case of the second peak (related to the butyral degradation). For the sample with 0.9 wt % f-SWCNTs, similar results were observed for the first peak, but smaller improvements in T_{onset} and T_{peak} were obtained for the second one (Table III).

The DSC data were consistent with the TG curves because the f-SWCNTs increased the T_{onset} and T_{max} for the degradation of the butyral ring (TGA curves). In the DSC curves, the second endothermic peak shifted to higher temperatures because of the incorporation of the nanotubes. In other words, the f-SWCNTs shifted the T_{onset} of the butyral ring degradation to higher temperatures and also lowered the quantity of the degradation. As a result, fewer enthalpies were observed. The data in Tables II and III prove this consistency. For example, according to the TGA curves, the sample containing 0.6% f- SWCNTs had a better

Table III. T_{onset} and T_{peak} Value and Enthalpy for the Pure PVB and Its Nanocomposites

Sample	PVB	PVB/0.6% f-SWCNTs	PVB/0.9% f-SWCNTs
T_{onset} (°C)[a]	335	351	349
T_{peak} (°C)[a]	338	358	360
Enthalpy (μV s/mg)[a]	101.0	47.6	23.8
T_{onset} (°C)[b]	356	410	366
T_{peak} (°C)[b]	361	412	383
Enthalpy (μV s/mg)[b]	107.9	8.4	7.2

[a] First endothermic peak.
[b] Second endothermic peak.

Table IV. Mechanical Properties of the PVB and PVB/f-SWCNT Samples

Mechanical property	PVB	PVB/0.6% f-SWCNTs	PVB/0.9% f-SWCNTs	PVB/0.6% SWCNTs	PVB/0.9% SWCNTs
Tensile modulus (MPa)	71 ± 1	205 ± 7	142 ± 3	192 ± 6	129 ± 3
Tensile strength (MPa)	9.2 ± 0.2	37.4 ± 1.4	19.9 ± 0.5	33.1 ± 1.6	15.8 ± 0.4
Flexural strength (GPa)	3.62 ± 0.13	14.23 ± 0.23	7.32 ± 0.26	13.00 ± 0.32	6.19 ± 0.14
Elongation at break (%)	136.1 ± 3.4	182.5 ± 5.9	140.2 ± 3.5	175.1 ± 4.2	122.7 ± 2.6
Toughness (J)	449.7± 12.4	2643.5 ± 34.2	1074.6 ± 20.3	2371.3 ± 32.6	810.1 ± 21.4

Corresponding data for the composites filled with the pristine SWCNTs are presented for comparison.

role in stabilizing the PVB as compared to the one filled with 0.9%. This trend could also be seen in the DSC curves. These results indicate that the functionalized nanotubes improved the thermal stability of the PVB resin very much.

Mechanical Properties

Table IV shows the mechanical properties of the PVB/f-SWCNT composite. The incorporation of the functionalized nanotubes to the PVB matrix increased the tensile strength and Young's modulus of the composites. When the f-SWCNTs content was 0.6 wt %, the tensile strength of the corresponding sample enhanced to 37.4 MPa (an increase of 310%), and the Young's modulus increased to 205 MPa (an increase of 190%). The composite containing 0.9 wt % f-SWCNTs exhibited 120 and 100% increases in the tensile strength and Young's modulus, respectively. The enhancement of the mechanical properties for the prepared composites is summarized in Table V.

The presented results show an increase in the flexural strength compared to the pure matrix. With the addition of f-SWCNTs to the PVB resin, the elongation at break of the prepared composites also increased. For the composites filled with 0.6 and 0.9 wt % f-SWCNTs, the elongation at break values increased 34 and 3% (Table V), respectively. As seen in the mentioned results, the fabricated composites had not only a higher stiffness but also a higher flexibility compared to the pure PVB.

PVB is a commonly used polymer for different applications, especially safety glasses and coatings. This resin possesses high adhesion to glass substrates, high stiffness, and good toughness. To investigate the toughness of the prepared composites, the area underneath the stress–strain curve was measured by a tensile tester. The toughness values of the samples containing 0.6 and 0.9 wt % f-SWCNTs were 487.8 and 139% higher than the virgin PVB, respectively. Therefore, the fabricated composites also had a suitable toughness in addition to a high stiffness.

As shown, the mechanical properties of the PVB improved remarkably with the presence of the f-SWCNTs. The high enhancement of the mechanical properties could be clarified by the unique mechanical and physical properties in combination with the high specific surface area and aspect ratio of the nanotubes. These factors resulted in good interaction between the functionalized nanotubes and the PVB matrix, and consequently, better stress transfer from the polymer to the filler was created. The obtained results also showed that similar to the our previous study[24] and other reports,[31–35] there was a critical nanotube loading in the PVB matrix, below which the reinforcing effect for nanocomposites increased with increasing nanotube content. This critical point for the f-SWCNTs in this study was about 0.9 wt %. For the composite with 0.9 wt % f-SWCNTs, the enhancing trend of the mechanical properties stopped, and a smaller improvement achieved. This finding was ascribed to the nonhomogeneous dispersion of the nanotubes and the agglomeration of the filler at high loading contents. The agglomeration decreased the interfacial adhesion between the nanotubes and the PVB matrix, and the nanotubes acted as stress concentration points.

The data presented in this article indicate that the role of the f-SWCNTs in reinforcing the mechanical properties of the PVB was better than that of the pristine SWCNTs (data reported elsewhere[24]). For instance, the Young's modulus and tensile strength of the composite with 0.6% f-SWCNTs was higher than those of the SWCNT/PVB composite with a similar nanotube content. As shown in Table V for the PVB/f-SWCNTs, 190 and 310% improvements in the Young's modulus and tensile strength, respectively, were achieved. In contrast, the modulus and tensile strength of the composite filled with pristine SWCNTs were improved by 170 and 260%, respectively.[24] At 0.9 wt %, the modulus and tensile strength for the samples filled with f-SWCNTs and unfunctionalized SWCNTs were enhanced by 100 and 120 and 82 and 72%, respectively. These results were repeated for the flexural strength, elongation at break, and toughness. These results indicate that the chemical functionalization of the nanotubes played a significant role in improving the mechanical properties of the composites. The polar functional groups, such as carboxylic acid and alcoholic groups,

Table V. Enhancement of the Mechanical Behavior of Composites Filled with the f-SWCNTs

Mechanical properties	0.6% f-SWCNTs	0.9% f-SWCNTs
Tensile modulus (%)	190	100
Tensile strength (%)	310	120
Flexural strength (%)	293	102
Elongation at break (%)	34	3
Toughness (%)	487.8	139

made the SWCNTs more compatible with the used solvent and the PVB resin. In other words, acid treatment of the SWCNTs increased the dispersion of the nanofiller and the interfacial adhesion and, as a result, provided more efficient load transfer between the nanofiller and the PVB. In general, the composites that had better interfacial strength demonstrated better results in improving the tensile properties of the composites. Therefore, the f-SWCNTs have larger potential to enhance the mechanical properties of PVB and other polymers.

CONCLUSIONS

PVB nanocomposites with the f-SWCNTs were produced by a solution casting method. The f-SWCNTs were prepared by the treatment of the nanotubes by a mixture of acids, and the formation of polar groups was evidenced by FTIR spectroscopy, EDS, and SEM measurements. Different tests indicated that the fabricated composites had excellent mechanical and thermal properties compared to the neat PVB. Tensile tests showed a significant improvement in the mechanical properties of the composites compared to the neat PVB. Also, the thermal stability of the PVB was enhanced significantly with the incorporation of a very small loading of the functionalized nanotubes. The TGA and DSC curves revealed that the f-SWCNTs retarded the thermal degradation of the polymer matrix, and as a result, the degradation temperatures shifted to higher values. These results also show the more efficient role of the f-SWCNTs in improving the thermal and mechanical behavior of the PVB resin relative to the pristine SWCNT. This was due to the better dispersion and higher interfacial adhesion between the f-SWCNTs and the polymer matrix, which arose from the functional groups formed after the acid treatment.

REFERENCES

1. Qian, D.; Wagner, G. J.; Liu, W. K.; Yu, M. F.; Ruoff, R. S. *Appl. Mech. Rev.* **2002**, *55*, 495.
2. O'Connell, M. J.; Boul, P.; Ericson, L. M.; Huffman, C. B.; Wang, Y. H.; Haroz, E.; Kuper, C.; Tour, J. M.; Ausman, K. D.; Smalley, R. E. *Chem. Phys. Lett.* **2001**, *342*, 265.
3. Cadek, M.; Coleman, J. N.; Barron, V.; Hedicke, K.; Blau, W. J. *Appl. Phys. Lett.* **2002**, *81*, 5123.
4. Sandler, J. K.; Pegel, W. S.; Cadek, M.; Gojny, F.; van Es, M.; Lohmar, J.; Blau, W. J.; Schulte, K.; Windle, A. H.; Shaffer, M. S. P. *Polymer* **2004**, *45*, 2001.
5. Coleman, J. N.; Cadek, M.; Blake, R.; Nicolosi, V.; Ryan, K. P.; Belton, C.; Fonseca, A.; Nagy, J. B.; Gun'ko, Y. K.; Blau, W. J. *Adv. Funct. Mater.* **2004**, *4*, 791.
6. Dong, B.; He, B. L.; Xu, C. L.; Li, H. L. *Mater. Sci. Eng. B* **2007**, *143*, 7.
7. Liu, J.; Rinzler, A. G.; Dai, H.; Hafner, J. H.; Bradley, R. K.; Boul, P. J. *Science* **1998**, *280*, 1253.
8. Zhang, X.; Sreekumar, T. V.; Liu, T.; Kumar, S. *J. Phys. Chem. B* **2004**, *108*, 16435.
9. Georgakilas, V.; Kordatos, K.; Prato, M.; Guldi, D. M.; Holzingger, M.; Hirsch, A. J. *Am. Chem. Soc.* **2002**, *124*, 760.
10. Datsyuk, V.; Kalyva, M.; Papagelis, K.; Parthenios, J.; Tasis, D.; Siokou, A. *Carbon* **2008**, *46*, 833.
11. Zhao, B.; Wang, J.; Li, Z. J.; Liu, P.; Chen, D.; Zhang, Y. F. *Mater. Lett.* **2008**, *62*, 4380.
12. Hajian, M.; Koohmareh, G. A.; Rastgoo, M. *J. Appl. Polym. Sci.* **2010**, *115*, 3592.
13. Fernandez, M. D.; Fernandez, M. J.; Hoces, P. *J. Appl. Polym. Sci.* **2006**, *102*, 5007.
14. Sita, C.; Burns, M.; Häβler, R.; Focke, W. W. *J. Appl. Polym. Sci.* **2006**, *101*, 1751.
15. Rasheed, A.; Chae, H. G.; Kumar, S.; Dadmun, M. D. *Polymer* **2006**, *47*, 4734.
16. Kim, H. S.; Chae, Y. S.; Choi, J. H.; Yoon, J. S.; Jin, H. *J. Adv. Compos. Mater.* **2008**, *17*, 157.
17. Meng, C.; Liu, C.; Fan, S. *Electrochem. Commun.* **2009**, *11*, 186.
18. Kashiwagi, T. E.; Grulke, J.; Hilding, R.; Harris, W.; Douglas, J. *Macromol. Rapid Commun.* **2002**, *232*, 761.
19. Hajian, M.; Reisi, M. R.; Koohmareh, G. A.; Jam, A. R. Z. *J. Polym. Res.* **2013**, *19*, 1.
20. Yang, B.; Liu, R.; Huang, J.; Sun, H. *Ind. Eng. Chem. Res.* **2013**, *52*, 7425.
21. Kuan, H. C.; Ma, C. C. M.; Chang, W. P.; Yuen, S. M.; Wu, H. H.; Lee, T. M. *Compos. Sci. Technol.* **2005**, *65*, 1703.
22. Naseh, M. V.; Khodadadi, A. A.; Mortazavi, Y.; Sahraei, O. A.; Pourfayaz, F.; Sedghi, S. M. *World Acad. Sci. Eng. Technol.* **2009**, *49*, 177.
23. Liau, L. C. K.; Yang, T. C. K.; Viswanath, D. S. *Polym. Eng. Sci.* **1996**, *36*, 2589.
24. Zanjanijam, A.; Hajian, M.; Koohmareh, G. A. *J. Macromol. Sci. Chem.*, DOI: 10.1080/10601325.2014.882703.
25. Van Krevelen, D. W.; Hoftyzer, P. J. Properties of Polymers, 3rd ed.; Elsevier Scientific: New York, **1976**.
26. Mallakpour, S.; Dinari, M. *J. Therm. Anal. Calorim.* **2013**. DOI: 10.1007/s10973-013-3587-0.
27. Mallakpour, S.; Zadehnazari, A. *J. Polym. Res* **2013**, *20*, 1.
28. Mallakpour, S.; Zadehnazari, A. *Polym. Bull.* **2013**, *70*, 3425.
29. Ugur, S. S.; Sarıısık, M.; Aktas, A. H. *Mater. Res. Bull.* **2011**, *46*, 1202.
30. Johnson, P. R. A. *J. Appl. Polym. Sci.* **1974**, *18*, 491.
31. Li, J.; Ma, P. C.; Chow, W. S.; To, C. K.; Tang, B. Z.; Kim, J. K. *Compos. Sci. Technol.* **2007**, *17*, 3207.
32. Ma, P. C.; Tang, B. Z.; Kim, J. K. *Carbon* **2008**, *46*, 1497.
33. Kosmidou, T. V.; Vatalis, A. S.; Delides, C. G. *Express Polym. Lett.* **2008**, *2*, 364.
34. Ma, P. C.; Liu, M. Y.; Zhang, H.; Wang, S. Q.; Wang, R.; Wang, K. *ACS Appl. Mater. Interface* **2009**, *1*, 1090.
35. Zanjanijam, A.; Bahrami, M.; Hajian, M. *J. Vinyl Add. Technol.*, to appear.